

From Solitary Waves to Static Patterns via Spatiotemporal Intermittency

F. Melo* and S. Douady†

Laboratoire de Physique de l'École Normale Supérieure de Lyon, 69364 Lyon Cedex 07, France

(Received 8 March 1993)

Among the very rich range of possibilities for the dynamics of one dimensional fronts, this article presents, in a film draining experiment, the first observation of a continuous transition from solitary waves to a static spatially periodic pattern. Between these two extreme situations, a regime of colliding solitary waves exhibiting chaos with spatiotemporal intermittency is observed. These observations suggest the description of the static periodic pattern as being the result of a dense packing of propagating solitary waves, and its destabilization to spatiotemporal intermittency as the attempt of some solitary waves to propagate.

PACS numbers: 47.52.+j, 47.20.Ma

The dynamics of one dimensional fronts has been widely investigated in many different systems, both experimentally and theoretically. A very rich range of possibilities exists: Deformations which can be static, oscillating or propagating, localized or extended, ordered or disordered, have been observed [1–5]. However, most of the descriptions are based on an ordered periodic deformation (with some possible defects), or on separated localized solutions. A link can be made between these two cases when some solitary waves propagating in the same direction are added together to form a periodic propagating pattern, as observed in the printer instability [6,7]. We report here the first observation, to our knowledge, of a continuous transition from localized *propagating* solitary waves to a *static* and spatially periodic pattern.

The experimental setup consists of a horizontal glass cylinder, which can be rotated around its axis at a variable speed ω in the range 0–20 rad/s. The cylinder, of length 56 cm and radius 5 cm, is closed at its extremities and partially filled with a viscous fluid. A large variety of dynamical regimes can be observed depending on the fluid volume used, its viscosity and, of course, the rotation velocity [8–11]. We used an oil having a viscosity $\nu=0.2$ cm²/s (Rhodorsil 47V20). The behavior we describe was observed with a fixed volume of oil, $V=135$ cm³, corresponding to a filling fraction of 3.1%. We will briefly describe later the behaviors for different volumes of oil.

For a small rotation rate, a part of the oil is dragged by viscosity, forming a thin film (of typical thickness 2 mm) covering the inner surface of the cylinder. The rest of the oil is also dragged by viscous friction, but the gravity generates a compensating downward flow. This part of the oil thus remains at the bottom of the upward moving wall. As shown in Fig. 1(a), this thicker region has a well defined front where the down-moving oil meets the thin reentering film [12]. For a small rotation rate, this front is perfectly horizontal (except close to the two boundaries), and is stable. For a large rotation rate, all the oil is dragged so that only the continuous film remains [13]. The interesting behaviors are observed between these two extremes.

In order to analyze the spatiotemporal behaviors we used a space-time reconstruction using a video recording of the front [6]. It consists of taking the same horizontal line in successive video frames and putting them one under the other. The line in the frame is chosen just above the flat front, so that each deformation is visible as a dark segment. By convention, time proceeds downwards.

Above a threshold value of the cylinder rotation velocity, $\omega_p=11.06$ rad/s, the straight front becomes unstable and forms solitary waves [cf. Fig. 1(b)]. They have a well-selected propagation velocity, amplitude, and shape. This shape is asymmetrical, in direct relation with the direction of propagation [14]. This instability is subcriti-

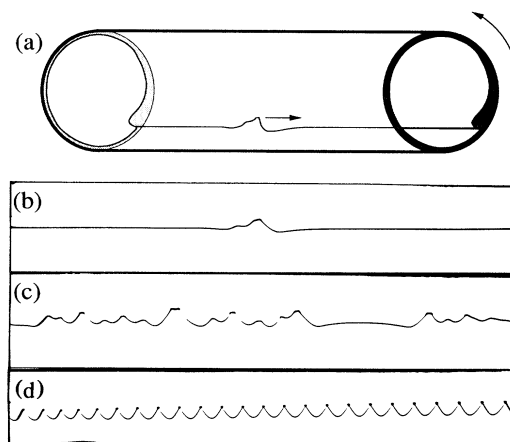


FIG. 1. (a) Sketch of the experiment. A cylinder is rotated horizontally around its axis at a radial velocity ω . It is partially filled with some oil forming a thin and continuous film, with a thicker part at the bottom of the cylinder. The front between the thicker part and the reentering film is unstable. (b)–(d) Photographs showing the front for three different rotation rates. (b) Solitary wave propagating to the right with its counter-propagating wave, visible as an oscillation of its back [see Fig. 3(a) and text], $\omega \approx 11.1$ rad/s. (c) Chaotic state with still some flat regions, $\omega \approx 11.6$ rad/s. (d) The final periodic and static pattern, $\omega \approx 13$ rad/s. Horizontal length is 26 cm for (b) and (c), 55 cm for (d).

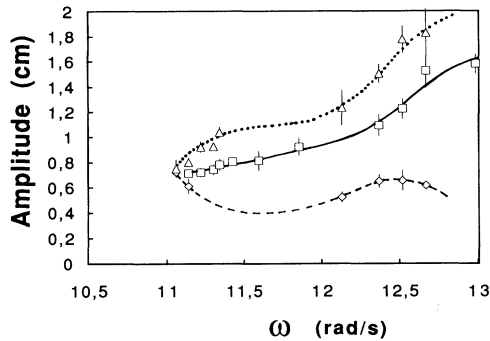


FIG. 2. At small rotation rates, subcritical solitary waves are observed. The full line shows their stable amplitude as a function of the rotation rate. During transients, one can measure the unstable stationary amplitude, below which the wave dies and above which it grows (dashed line). When growing, these waves reach a maximum amplitude (dotted line), which finally decreases to the stable amplitude as they emit the backward wave. At large rotation rates, a nearly static pattern is observed. The squares now show the stable amplitude of this pattern, while the dotted line shows the amplitude above which a cusp breaks in two, increasing the wave number, while the dashed line shows the amplitude below which one cusp disappears and above which it increases again.

cal (cf. Fig. 2). The solitary waves are spontaneously created at the two lateral boundaries. At each closing wall, a "finger" of oil oscillates vertically and thus generates a propagating wave. Generally this wave is strongly damped (in less than five wavelengths). But when a maximum of this wave exceeds a critical height, it is locally amplified into a solitary wave [cf. Fig. 3(a)]. The formation mechanism of these solitary waves could be related to the fact that the front disappears when the rotation rate is increased (or also for the same rotation rate but a smaller oil volume). Close to this transition, the system prefers to vary its local volume of oil, so that one part presents a vanishing front with less oil, and another part a more stable front with more oil [12]. A solitary wave as in Fig. 1(a) does correspond to a local modulation of the oil volume, with a larger amount of oil (the protruding part) followed by a smaller amount (the cusp) [15].

Two characteristics are important to understand the dynamics of these solitary waves:

Slightly above the threshold ($\omega \approx 1.02\omega_p$), the cusp of a solitary wave starts to oscillate and to emit a wave, which is strongly damped. It propagates with nearly the same velocity as the solitary wave, but in the opposite direction (in the reference frame of the laboratory) [cf. Fig. 1(b)]. Far above the threshold, the backward wave becomes large enough to generate spontaneously new counterpropagating solitary waves (cf. Fig. 4).

Two solitary waves repel each other strongly when closer than a distance of approximately their own size. When the waves propagate in the same direction this

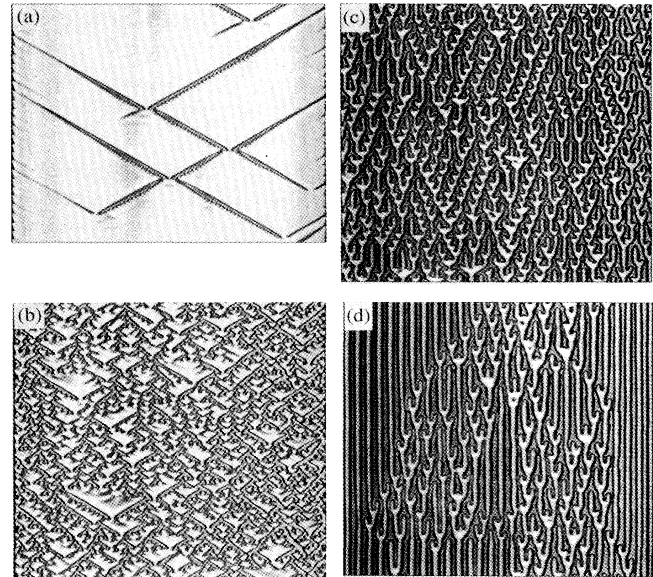


FIG. 3. Space-time reconstruction showing the behavior of the front for several rotation rates. *Time is pointing down.* (a) $\omega \approx 11.1$ rad/s; the backward wave is responsible for the clogged aspect of the solitary waves traces. (b) $\omega \approx 11.7$ rad/s. (c) $\omega \approx 12.3$ rad/s; some coherent bouncing oscillations between several solitary waves are visible. (d) $\omega \approx 12.9$ rad/s $\leq \omega_s$. The width of each image corresponds to the whole length of the cylinder (56 cm). The vertical time scale is constant, giving a total length of ≈ 32 s for (b)-(d).

repulsion determines their minimum distance.

These two characteristics are involved in the collision of two contrapropagating solitary waves, a process essential for the front dynamics. During a collision, the two solitary waves, due to their repulsion, slow down, stop, and vanish *without interpenetrating each other*. But the overall result of the collision depends on their backward waves. They are amplified by the collision and, if one of these reaches a critical amplitude, it is transformed into a new solitary wave. Several results of a collision are thus possible, depending on the amplitudes of the solitary waves and the associated backward waves: Zero, one, or two solitary waves can be regenerated [cf. Fig. 3(a)]. At large rotation rates, the collision always leads to the regeneration of two solitary waves.

Close to the threshold, a few solitary waves can be observed from time to time [cf. Fig. 3(a)]. By increasing the rotation rate, their number increases. The front also starts to present a complex chaotic shape where no particular structure can be distinguished by direct inspection [cf. Fig. 1(c)]. With the spacetime reconstruction, this chaotic state is directly analyzed as resulting from the dynamics of many solitary waves: It is a regime of perpetually colliding, disappearing, and reappearing solitary waves [cf. Fig. 3(b)]. For a still larger rotation rate, some regions become static for a finite time [cf. Fig.

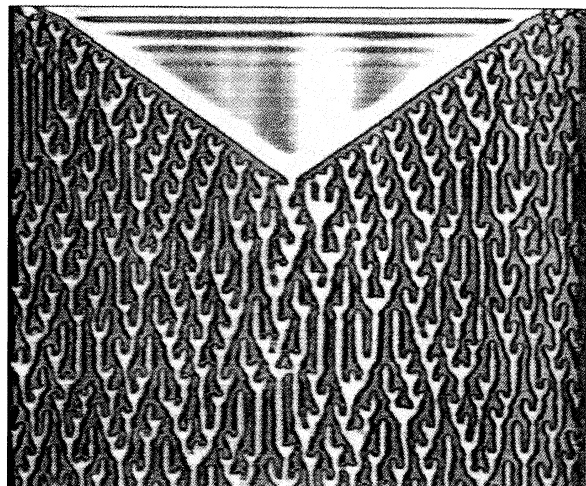


FIG. 4. Transient observed when the rotation rate is increased suddenly from a value just under the threshold ω_p to $\omega \approx 12.5$ rad/s, showing the propagation of two solitary waves at a large velocity (2.17 cm/s). Same scales as Fig. 3.

3(c)]. They are formed of regularly spaced “fingers” of oil, each being separated from its neighbor by a cusp [16]. By increasing the rotation rate, the spatial and temporal extensions of these regions increase. A stationary spatiotemporal intermittent regime of coexisting static and chaotic regions is thus observed.

Finally, when the rotation rate is increased above a second threshold, $\omega_s = 12.98$ rad/s, the whole front forms a perfectly static and periodic pattern [cf. Fig. 1(d)]. As stated above, if the rotation rate is even further increased (in fact only slightly above ω_s), the front disappears and there remains only a continuous and fluctuating film. Let us add here that for a smaller oil volume (under $V \approx 120$ cm³, filling fraction 2.7%), a long wavelength instability first appears which perturbs the propagating solitary waves, and the front disappears before reaching the stationary pattern. For a larger oil volume (above $V \approx 150$ cm³, filling fraction 3.4%), a subcritical transition toward a stationary pattern is directly observed from the linear front with no intermediate regime of solitary waves.

In our case, we observe that *the transition from the propagating solitary waves to the static pattern is continuous*. If the state is characterized by the density of disappearance of solitary waves (or equivalently the number of reappearances) in the space-time images, this quantity vanishes approximately linearly at the transition. The first consequence of the increased robustness of the solitary waves is a more frequent generation of counter-propagating ones and thus an increase of the number of solitary waves (which saturates to the number of wavelengths in the final static pattern). But it also induces an increase of the collision duration. As the collisions are more and more likely, and as their mutual repulsion is strong enough to forbid interpenetrating, this results in a

global slowing down of all the solitary waves (cf. Fig. 3). Finally, at large rotation rates, a local equilibrium is reached where they remain motionless (each cusp of the static pattern corresponding to an immobilized solitary wave).

This interpretation is strengthened by the fact that, even for these large rotation rates, the free propagation of solitary waves can still be observed during transients (cf. Fig. 4). If the rotation rate is suddenly increased from a value below the first threshold ω_p to a larger final value, the propagation of a solitary wave coming from each boundary is observed. Using such transients, we were able to measure the propagation velocity of a free solitary wave for any rotation rate. This velocity decreases regularly with increasing rotation rate. But it remains high, even for the rotation rate where a static pattern is observed: Its value is 2.02 cm/s only 20% lower than the value at threshold, 2.62 cm/s. Thus the formation of a static pattern from a collection of solitary waves cannot be explained simply by a vanishing propagation velocity of the solitary waves. It is explained only by the mutual repulsion of these solitary waves leading to their blocking.

As stated above, the system presents an intermittent spatiotemporal behavior just below the second threshold ω_s : some parts of the pattern are already static, while other parts are still showing chaotic behavior. Figure 3(d) shows that the interaction between the chaotic and the static regions is complex, with invasion, propagation, and restabilization. This situation recalls the dynamics observed in other systems [7,17]. For a value just above ω_s , the transition to a static pattern is rather brutal, with the sudden stabilization of the last chaotic region. The destabilization of the static pattern when the rotation rate is reduced is symmetrical: A part of the pattern suddenly breaks into chaos. This destabilization is first observed as a variation in the local amplitude, one cusp becoming large and its neighbor becoming small. When the small cusp disappears, the large one starts to propagate in the empty place and generates another cusp (cf. Fig. 2). This dynamic is identical to that of a solitary wave generating a counterpropagating one.

From our point of view, the main interest of this experiment is thus to suggest the description of some static periodic patterns as a dense packing of propagating solitary waves immobilized by their mutual repulsion. Their destabilization to spatiotemporal intermittency is then naturally interpreted as resulting from the attempt of each solitary wave to propagate whenever the local equilibrium is broken. We are confident that the general idea of considering some periodic patterns, not as a whole but constituted of a packing of localized structures, could help to understand some of their particular dynamics.

*Present address: Center for Non-Linear Dynamics, University of Texas, Austin, Texas 78712.

†Present address: Laboratoire de Physique Statistique,

- ENS, 24 rue Lhomond, 75235 Paris Cedex 05, France.
- [1] For a review see M. C. Cross and P. C. Hohenberg, *Rev. Mod. Phys.* (to be published).
- [2] See also J. M. Flesselles, A. J. Simon, and A. J. Libchaber, *Adv. Phys.* **40**, 1–51 (1991).
- [3] *Spontaneous Formation of Space-Time Structures and Criticality*, edited by T. Triste and D. Sherrington, NATO ASI, Ser. C, Vol. 349 (Kluwer, Dordrecht, 1991).
- [4] *Nonlinear Evolution of Spatio-Temporal Structures in Dissipative Continuous Systems*, edited by F. H. Busse and L. Kramer, NATO ASI, Ser. B, Vol. 225 (Plenum, New York, 1990).
- [5] *Propagating in Systems far from Equilibrium*, edited by J. E. Weisfreid, H. R. Brand, P. Manneville, G. Albinet, and N. Boccara, Springer Series in Synergetics Vol. 41 (Springer, Berlin, 1988).
- [6] M. Rabaud, S. Michalland, and Y. Couder, *Phys. Rev. Lett.* **64**, 184–187 (1990).
- [7] Y. Couder, S. Michalland, M. Rabaud, and H. Thomé, in *Nonlinear Evolution of Spatio-Temporal Structures in Dissipative Chaotic Systems* (Ref. [4]), pp. 487–497.
- [8] R. T. Balmer, *Nature (London)* **227**, 600–601 (1970).
- [9] M. J. Karweit and S. Corrsin, *Phys. Fluids* **18**, 111–112 (1975).
- [10] T. B. Benjamin and S. K. Pathak, *J. Fluid Mech.* **183**, 399–420 (1987).
- [11] L. Preziosi and D. D. Joseph, *J. Fluid Mech.* **187**, 99–113 (1988).
- [12] F. Melo, *Phys. Rev. E* **48**, 2704 (1993).
- [13] K. Moffatt, *J. Mech.* **16**, 651–673 (1978).
- [14] See, for instance, S. Fauve, S. Douady, and O. Thual, *J. Phys. II (France)* **1**, 311–322 (1991); or P. Couillet and G. Ioss, *Phys. Rev. Lett.* **64**, 866–869 (1990).
- [15] A solitary wave, however, corresponds globally to a small lack of oil.
- [16] In an oil finger, the flow parallel to the cylinder surface consists of two counterrotating vortices. The flow between two fingers then recalls the situation studied by J.-T. Jeong and H. K. Moffat, *J. Fluid Mech.* **241**, 1–22 (1992), where they obtain and explain the presence of a cusp, particularly at such small Reynolds numbers. A solitary wave corresponds to the same flow with just a horizontal velocity added. The existence on each side of a cusp of two counterrotating vortices could explain the strong mutual repulsion between two solitary waves.
- [17] For a review see H. Chaté, in *Spontaneous Formation of Space-Time Structures and Criticality* (Ref. [3]), pp. 273–311.

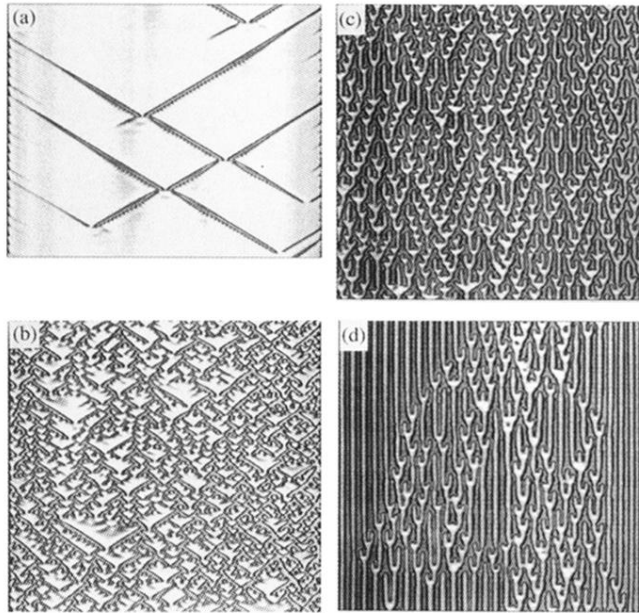


FIG. 3. Space-time reconstruction showing the behavior of the front for several rotation rates. *Time is pointing down.* (a) $\omega \approx 11.1$ rad/s; the backward wave is responsible for the cogged aspect of the solitary waves traces. (b) $\omega \approx 11.7$ rad/s. (c) $\omega \approx 12.3$ rad/s; some coherent bouncing oscillations between several solitary waves are visible. (d) $\omega \approx 12.9$ rad/s $\leq \omega_s$. The width of each image corresponds to the whole length of the cylinder (56 cm). The vertical time scale is constant, giving a total length of ≈ 32 s for (b)–(d).

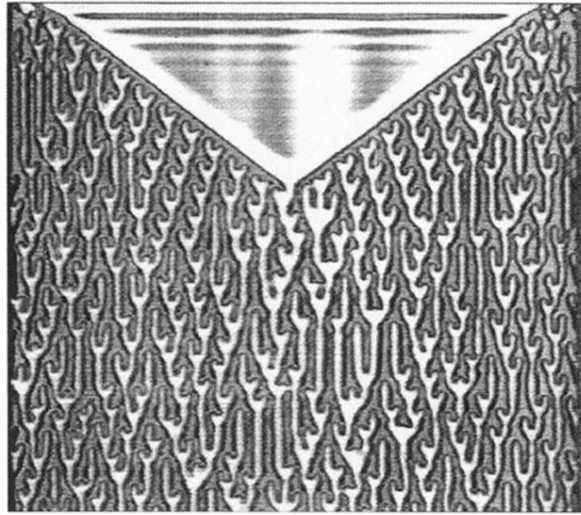


FIG. 4. Transient observed when the rotation rate is increased suddenly from a value just under the threshold ω_p to $\omega \approx 12.5$ rad/s, showing the propagation of two solitary waves at a large velocity (2.17 cm/s). Same scales as Fig. 3.